Theoretical Reaction Dynamics Study of the Effect of Vibrational Excitation of CO on the OH + CO → H + CO_2 Reaction†

Rosendo Valero and Geert-Jan Kroes*

Leiden Institute of Chemistry, Gorlaeus Laboratories, Leiden University, P.O. Box 9502, 2300 RA Leiden, The Netherlands

Received: March 15, 2004; In Final Form: June 23, 2004

The OH + CO → H + CO_2 reaction has received a great deal of attention in recent years, being presently the prototypical complex-forming four-atom reaction. An interesting issue is the extent to which the vibration of the nonreactive CO bond acts as a spectator in the reaction. To get insight into this question, we report a study of the reactivity of the ground ($v = 0$, $j = 0$) and first excited vibrational state ($v = 1$, $j = 0$) of CO with the OH diatom in its ground rovibrational state ($v = 0$, $j = 0$). For these reactions, the time-dependent wave packet (TDWP) method was used to calculate exact, full-dimensional (6D) initial-state selected reaction probabilities on the Bradley-Schatz potential energy surface (PES), for total angular momentum $J = 0$. An approximate diabatic (potential-averaged five-dimensional, PA5D) model was also used, in which the 6D potential is averaged over one asymptotic CO vibrational wave function. The results show a large increase in reactivity upon vibrational excitation of CO, particularly in the 6D model. A comparison of the 6D results with the diabatic PA5D results for CO ($v = 1$), as well as the analysis of the potential curves constructed according to an adiabatic 5 + 1D model, reveal that this effect is mostly due to vibrationally inelastic energy transfer from the CO bond to the reaction coordinate. The reactivity of CO ($v = 1$) is much higher in the 6D than in the PA5D model. These findings allow us to conclude that the CO bond does not act as a spectator in the reaction. Finally, the quasiclassical trajectory (QCT) method was employed on the above-mentioned Bradley-Schatz PES, as well as on the most recent PES (LTSH). The QCT method is able to predict quite well the difference between the 6D and PA5D reaction probabilities for CO ($v = 1$) obtained with the TDWP method on the BS PES. The PA5D QCT results are also in good agreement with 6D and PA5D TDWP results for reaction of CO ($v = 0$) and for the BS PES. The large differences found between QCT reaction probabilities for CO ($v = 1$) in the 6D and the PA5D model, on one hand, and the large differences between 6D QCT results for CO ($v = 1$) and PA5D QCT results for CO ($v = 0$), on the other hand, for the LTSH PES, strongly suggest that our conclusion (CO does not act as a spectator) can be generalized to this newer PES.

Introduction

The OH + CO → H + CO_2 reaction is among the most extensively studied four-atom reactions. This interest has been prompted by the fundamental importance of the reaction in the chemistry of the troposphere,[1] in combustion processes,[2] and in astrophysical ices.[3] Thus, many experimental studies of the kinetics and dynamics of the OH + CO reaction have been reported.[4−24] The reaction is a prototype of bimolecular complex-forming reactions with participation of a radical species (OH), in which the internal states of both reactants can influence the reactivity. A large body of information now exists on the thermal rate constants of the reaction, for an extended range of temperature and pressure conditions (80−2800 K; 10^{-4}−700 bar).[11] The rate constants present an unusual temperature dependence, leveling off at temperatures below 500 K and rising steeply at higher temperatures. A reaction mechanism, including formation of a stable reaction complex, was proposed many years ago to explain the observed kinetics.[25] The existence of the complex has been confirmed, and its properties determined, in numerous experiments carried out in the gas phase[26−31] and in solid matrixes.[32−34] Furthermore, previous dynamic studies of the OH + CO reaction[35] have shown that in more than half of the reactive events a collision complex is formed that exists for longer than 100 fs, up to large collision energies (≈0.8 eV). In a recent set of experiments, it has been found that linear hydrogen-bonded complexes detected in the OH−CO asymptotic region could be relevant to the reactivity of OH + CO.[17,18,21,23,24] Studies of the kinetics of the reaction on model potential energy surfaces (PESs), based on the statistical Rice-Ramsperger-Kassel-Marcus (RRKM) theory, have afforded a good prediction of the available experimental rate constants.[11,12,36] Some experimental studies have also reported state-specific rate constants for vibrationally excited states of OH[5] and CO.[37,38] While the vibrational excitation of OH produces a large increase in the rate constant,[5] in our view the experiments on vibrationally excited CO do not yet allow definite conclusions on the relative reactivity of ground and excited-state CO[37,38] (see below).

Reaction dynamics measurements of several properties, such as absolute cross sections,[10] product angular and translational distributions,[8] and energy partitioning in the reaction,[7] have provided detailed information with which to refine the HOCO potential surface. The first global analytical PES was that

† Part of the "Gert D. Billing Memorial Issue".

* To whom correspondence should be addressed. Phone: +31 71 5274396 Fax: +31 71 5274488 E-mail: g.j.kroes@chem.leidenuniv.nl.

10.1021/jp048855b CCC: $27.50
Published on Web 08/04/2004

reported by Schatz, Fitzcharles, and Harding (SFH).[39] Several improvements were made over the years as more accurate electronic structure calculations became possible. The most recent potential surfaces are those of Bradley and Schatz (BS),[40] of Yu, Muckerman and Sears (YMS),[41] and of Lakin, Troya, Schatz, and Harding (LTSH).[42] Many dynamical studies employing the quasiclassical trajectory (QCT) method,[35,42,43] quantum reduced-dimensional,[44−52] and mixed quantum-classical methods[53−55] have been performed on these PES's. Only very recently, the first full-, six-dimensional quantum dynamics studies of the reaction have been reported.[56−58] The extreme computational challenge posed by exact quantum dynamical calculations on the OH + CO reaction can be understood from the presence of the intermediate complex in the reaction path and of three heavy (non-hydrogen) atoms. Thus, large basis sets and propagation times must be used to yield converged reaction probabilities.

The purpose of this study is to provide an accurate account of the role of the vibration of the nonreactive CO bond in the reactivity of OH + CO. In particular, we address the question of the extent to which the CO bond acts as a spectator in the reaction. To this aim, we have used the time-dependent wave packet (TDWP) method to obtain exact, six-dimensional (6D) and approximate, potential-averaged five-dimensional (PA5D)[59,60] initial state-selected reaction probabilities for the reaction of OH ($v = 0$, $j = 0$) with CO ($v = 1$, $j = 0$), and for angular momentum $J = 0$. The BS potential surface was used in all the quantum dynamics calculations. We believe that the reported TDWP 6D calculation of CO ($v = 1$) is the first exact quantum dynamics calculation from an excited state of the reactants of a four-atom system involving three heavy atoms. The 6D and PA5D reaction probabilities for CO ($v = 1$) are compared between them and to our previously reported 6D and PA5D results for the reaction of OH ($v = 0$, $j = 0$) with CO ($v = 0$, $j = 0$).[58] In previous studies of the OH + H_2[59] and H_2 + CN[60] reactions, this kind of comparison was made to conclude that the nonreactive bond (OH and CN, respectively) acts as a spectator as far as total reaction probabilities and cross sections are concerned.

In the present work, the nonreactive CO bond will be said to act as a spectator if (i) the total reaction probability does not show a large dependence on the initial vibrational state of CO,[61] and (ii) the total reaction probability can be accurately obtained applying the PA5D approach,[59−60] also for vibrationally excited CO. In our definition, we only consider the total reaction probabilities; four-atom reactions in which the nonreactive bond behaves as a spectator also with respect to state-to-state reaction probabilities are unusual, one example being the H_2 + OH reaction.[62] In this regard, note that effects of the nonreactive bond on product state-specific reaction probabilities, as found in, for instance, the H_2 + CN reaction,[63] may depend on the vibrational couplings occurring after the reaction barrier has been crossed. The TDWP results presented below show that the reactivity of CO ($v = 1$) must be studied with the full 6D model, and that in this model it is much larger than the reactivity of CO ($v = 0$). These results allow us to conclude that CO is not a spectator in the OH + CO reaction. Additional 6D and PA5D quasiclassical trajectory (QCT) calculations, carried out on both the BS and LTSH PES's, strongly suggest that this conclusion does not depend on which of the potential surfaces is used.

The paper is organized as follows. First, we describe the TDWP and QCT methods as used in this work. Next, the new TDWP results for CO ($v = 1$) are presented and compared with QCT results and with previous results for CO ($v = 0$) on the BS PES. The reaction mechanism is discussed and results are also reported for the newest LTSH PES. Finally, conclusions are drawn.

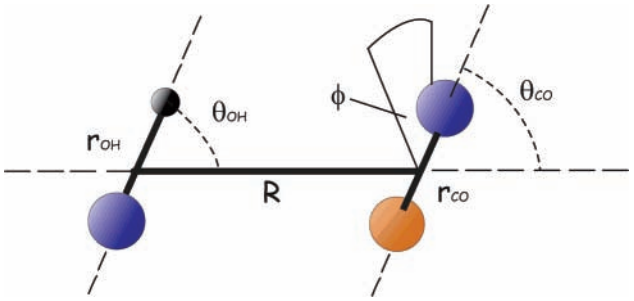

Figure 1. Reactant Jacobi coordinate system used to define the OH + CO Hamiltonian for $J = 0$. In the figure, R is the distance along the body-fixed axis connecting the centers of mass of the diatoms, r_{OH} and r_{CO} are the diatomic bond distances, θ_{OH} and θ_{CO} are the polar angles between the OH and CO diatom axes on one hand, and the body-fixed axis on the other hand, and ϕ is the dihedral azimuthal angle between the OH and CO diatoms with respect to rotation around the body-fixed axis.

Computational Methods

The TDWP method as implemented by us has been described elsewhere[51,58] and only a brief description will be given here. The nuclear Hamiltonian of the HOCO system is set up in a set of six reactant Jacobi coordinates, for total angular momentum $J = 0$ (Figure 1). The usual choice of ignoring the electronic (orbital and spin) angular momenta of the OH ($X^2\Pi$) molecule has been adopted.[48,59] As mentioned above, the reactions studied are OH ($v = 0$, $j = 0$) + CO ($v = 0$, $j = 0$) and OH ($v = 0$, $j = 0$) + CO ($v = 1$, $j = 0$), although new results are only presented for the latter. Two types of models were used, in which the potential was treated differently. In the 6D model, the full six-dimensional BS PES was employed, while in the potential-averaged five-dimensional (PA5D) model,[59] effective diabatic five-dimensional potentials were defined as averages of the 6D potential over either the ground ($v = 0$) or the first vibrationally excited state ($v = 1$) wave function gas-phase CO.

The representation of the total wave function uses the projection operator formalism.[64] This formalism involves two different representations in the asymptotic reactant channel (R), and in the region of the HOCO well up to the product channel (P). The advantage of using this formalism is that different representations and sizes of the basis sets can be used for each channel, allowing for a reduction in the size of the total wave function and in computational time. Thus, the orientation of the reactants was described in different finite-basis representations (FBRs)[65] in the R and P channels, consisting of mutual eigenfunctions of the angular momentum operators $\mathbf{j}_{OH}$, $\mathbf{j}_{CO}$, and $\mathbf{j}_{OH,CO}$,[66] which were transformed to and from the corresponding discrete variable representations (DVRs) to carry out the potential operation. Likewise, translational motions are represented on Fourier sets of basis functions (FBR) or on the associated grid points (DVR). The representation of the vibrational degrees of freedom is based on a Lanczos-Morse generalized DVR (GDVR) representation, in which the number of grid points is larger than the number of basis functions.[58,67] Furthermore, two different GDVRs represent the CO vibration in the R and P channels, while the OH stretch is represented with a GDVR in the R channel and with a Fourier FBR/DVR in the P channel.[58] Therefore, all degrees of freedom of the system have their representations tailored to the qualitatively different (R or P) regions of the potential, allowing for an

TABLE 1: Parameters for the 6D TDWP CO ($\nu = 1$) Calculation on the BS Potential Surface[a]

wave function parameters	projection operator representation	
	P	R
maximum j_{OH} in rotational basis	40	30
maximum j_{CO} in rotational basis	100	90
energy cutoff parameter for rotational basis	1.10	1.10
number of rotational basis functions	65 366	31 610
number of points for Fourier DVR in R	32	256
range of Fourier points in R	3.00−4.84	3.00−18.14
number of points for r_{OH}	32	6
range of Fourier points in r_{OH}	1.20−5.46	-
number of points for r_{CO}	14	10
propagation time step	10.0	10.0
analysis time step	120.0	120.0
range of optical potential in R	-	15.5−18.2
amplitude of optical potential in R (eV)	-	0.24
range of optical potential in r_{OH}	4.8−5.6	-
amplitude of optical potential in r_{OH} (eV)	2.65	-
center of initial wave packet	-	14.2
energy range of initial wave packet (eV)	-	0.1−0.8
analysis cut in r_{OH}	4.64	-
number of DVR points for the flux analysis in R	12	-
size of wave function in the primary representation	9.4×10^8	4.9×10^8

[a] Atomic units are used throughout except when stated otherwise.

efficient description of the TDWP dynamics. The initial Gaussian wave packet is evolved in time by using a split-operator propagator.[68] Optical potentials[69] are introduced to absorb the wave packet at the edges of the grid employed to represent the wave function. After propagation of the wave packet, the initial (energy-dependent) state-selected total reaction probabilities are extracted using the flux operator formalism.[59,70]

The parameters defining the representation of the wave function for the 6D CO ($\nu = 1$) calculation are detailed in Table 1. The parameters for the PA5D calculation are the same, except that only one basis function was used for the CO bond vibration. The total size of the wave function for the 6D model was 6.9×10^8 for the reported CO ($\nu = 0$) calculation[58] and 1.4×10^9 for the new calculation on CO ($\nu = 1$). Due to the huge size of the wave functions and to the long propagation times required (approximately 2.3 ps), it was necessary to devise a suitable parallelization strategy to reduce the wall-clock time spent by the 6D calculations. Here, and in our previous reports on OH + CO,[51,56,58] we have used the OpenMP protocol[71] to parallelize our wave packet code. In our previous research, the parallelization was effected mainly by distributing the different operations to the processors according to the elements of the Fourier grids in the R translational coordinate. In this manner, each processor managed approximately N_{grid}/N_{proc} elements of the total wave function, where N_{grid} is the number of grid points and N_{proc} is the number of processors. For the 6D CO ($\nu = 1$) calculation presented here, we found that a more suitable strategy was to effect a distribution over the rotational basis functions. This choice permitted a considerable reduction in wall-clock time, as compared to the previous choice of parallelizing the calculation over the R coordinate, for this specific calculation. The cost of the 6D CO ($\nu = 0$) and CO ($\nu = 1$) calculations on a modern 1 Gflop/s/processor SGI Origin 3800 supercomputer was about 100 000 and 200 000 CPU hours, using 64 and 80 processors in parallel, respectively. The extreme computational expense of these full-dimensional calculations, even for $J = 0$, is an additional reason to find suitable approximations to the dynamics of OH + CO; for example, using the PA5D model instead of the full 6D model if it provides accurate reaction probabilities for a particular initial state of reactants.

Additional quasiclassical trajectory (QCT) 6D and PA5D calculations were performed with the VENUS'96 general chemical dynamics code.[72] The PA5D calculations involved a modification of the program, in which the CO bond is effectively kept fixed along the trajectories by adding a high-frequency harmonic potential to the PA5D potential.[73] As stated above, one of the goals of the QCT calculations was to assess whether the main conclusions derived for the BS PES would also hold for the most recent (LTSH) PES. The differences in the LTSH PES with respect to the previous BS PES are an improved description of the asymptotic region and the scaling of the energies of several stationary points, both based on high-level ab initio data. As we will show, the QCT calculations also provide interesting information for which vibrational state and in which model the QCT method yield a good prediction of the TDWP quantum reaction probabilities for the reaction of CO (ν , $j = 0$) with OH ($\nu = 0$, $j = 0$).

Results and Discussion

1. Quantum and Classical Dynamics: CO ($\nu = 1$) vs CO ($\nu = 0$). In Figure 2 the 6D and PA5D probabilities for reaction of CO ($\nu = 0$) (Figure 2 (a)) and CO ($\nu = 1$) (Figure 2 (b)) on the BS PES are presented, as obtained with the quantum (TDWP) and classical (QCT) dynamical methods. The resonances observed in all the TDWP curves are due to relatively long-lived quasibound states associated with the HOCO complex. The properties of these resonance states have been analyzed using reduced-dimensional models.[46,50] As we found in our previous research,[56,58] the 6D and PA5D reaction probabilities for CO ($\nu = 0$) (Figure 2 (a)) are in almost quantitative agreement throughout the extended range of collision energies studied (0.1−0.8 eV), apart from details associated with resonances. The behavior of the CO ($\nu = 1$) reaction is markedly different, the 6D model predicting significantly larger reaction probabilities than the PA5D model (Figure 2 (b)). The relative increase in reactivity in the 6D model at the lowest collision energies (0.1−0.2 eV) is about a factor of 4, on average. Since the reaction from one particular vibrational state of the CO bond ($\nu = 1$) cannot be described accurately by the PA5D model, criterion (ii) above is not fulfilled and one

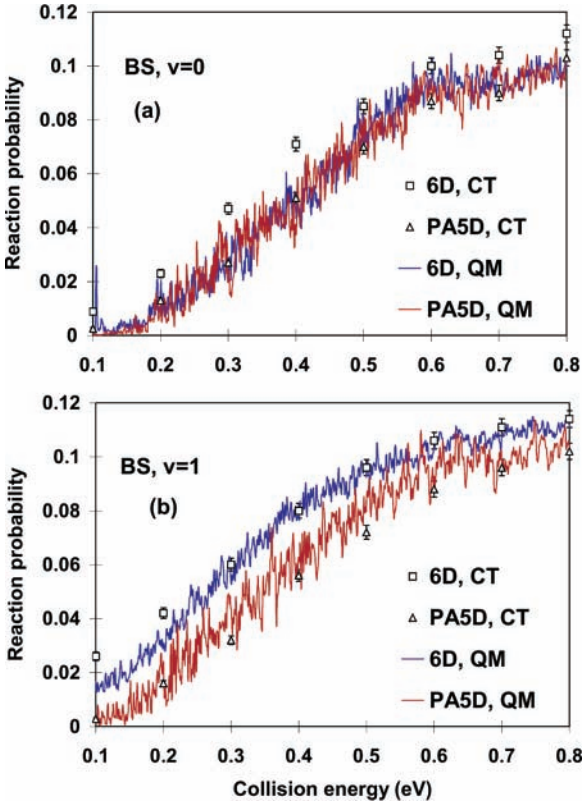

Figure 2. Reaction probabilities for the BS PES. **(a)** Results for CO ($\nu = 0$) in the 6D model (TDWP results (QM) in blue, open squares for QCT results (CT)), and in the PA5D model (TDWP results in red, open triangles for QCT results). **(b)** Results for CO ($\nu = 1$) in the 6D model (TDWP results (QM) in blue, open squares for QCT results (CT)), and in the PA5D model (TDWP results in red, open triangles for QCT results). The energy increment between consecutive data points in the TDWP calculations is always 0.32 meV, except for the 6D CO ($\nu = 1$) curve, for which it is 0.64 meV. Error bars correspond to two standard deviations for 10 000 trajectories/energy.

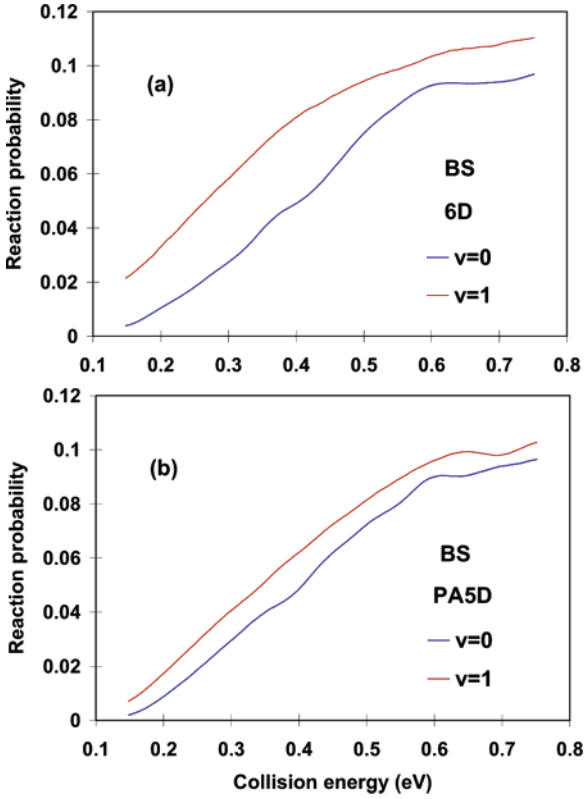

Figure 3. Gaussian-smoothed TDWP reaction probabilities for the BS PES. **(a)** Results in the 6D model for CO ($\nu = 0$) (blue line), and for CO ($\nu = 1$) (red line). **(b)** Results in the PA5D model for CO ($\nu = 0$) (blue line), and for CO ($\nu = 1$) (red line). The energy increment between consecutive data points in the original TDWP calculations is always 0.32 meV except for the 6D CO ($\nu = 1$) curve, for which it is 0.64 meV.

can conclude that the CO bond does not act as a spectator in the OH + CO reaction.

Figure 2 also offers a view of the performance of the QCT method in the reaction dynamics. For CO ($\nu = 0$) (Figure 2 (a)), the 6D QCT results overestimate the exact 6D TDWP reaction probabilities, while the PA5D results obtained with these two methods are in fairly good agreement. In contrast, the QCT method yields a much better prediction of the quantum results for CO ($\nu = 1$) in both the 6D and the PA5D model (Figure 2 (b)). The failure of the 6D QCT method concerning the 6D reaction probabilities for CO ($\nu = 0$) is most likely due to the well-known zero-point energy (ZPE) conservation problem. The presence of such an effect in the OH + CO reaction is borne out by a recent QCT study using the LTSH potential surface,[42] in which ZPE violation problems caused an unphysical increase of the total energy in the normal modes of the CO_2 product. The authors also found that the 6D QCT reaction probabilities for CO ($\nu = 0$) are larger than the 6D TDWP ones, especially at low collision energies. The poor performance of the QCT 6D model for the reaction of CO ($\nu = 0$) is consistent with the relatively low vibrational frequency of CO (0.27 eV), facilitating the coupling to other degrees of freedom to which part of the vibrational energy (for $\nu = 0$, the ZPE) can flow. This problem is not present in the QCT PA5D model, which shows a remarkably good performance for this reaction (Figure 2 (b)), and is apparently much less severe in the QCT 6D model for the CO ($\nu = 1$) reaction (Figure 2 (b)). A possible problem with ZPE in OH does not manifest itself in the reactivity of OH + CO, presumably due to the larger frequency of the OH bond (0.46 eV) and perhaps also to the fact that this bond needs to be broken anyway at the most important, exit channel barrier for reaction to occur.

The much better performance of the QCT 6D model observed here for reaction of a vibrationally excited (CO ($\nu = 1$)) reactant than that found for the ground-state (CO ($\nu = 0$)) reactant is in line with reports for D + H_2 ($\nu = 0, 1$; $j = 0$)[74] and Li + HF ($\nu = 0, 1$; $j = 0$),[75−76] and with the agreement between QCT and quantum-mechanical (QM) results in inelastic processes at high vibrational excitation of reactants as in, for example, He + CS_2.[77] In contrast, studies in which the agreement between QCT and QM results is better for a ground state than for a vibrationally excited reactant are rare, and the only example we know is for the reaction for which classical-like behavior should be least expected, that is, H + H_2 ($\nu = 0, 1$).[78]

The TDWP reaction probability curves shown in Figure 2 above are convoluted with a Gaussian function with a *fwhm* of 50 meV and presented in Figure 3. This figure focuses on a comparison between the two models (6D and PA5D) used in the TDWP calculations. The results show a large increase in reactivity upon vibrational excitation of the CO bond in the 6D model, and a moderate increase in the PA5D model. These results evidence that the CO ($\nu = 1$) dynamics can only be treated accurately by performing a full-dimensional 6D calculation. A comparison of the relative reactivity of ground and excited-state CO afforded by the TDWP method with the QCT results for the 6D model was not deemed meaningful, due to the poor performance of the QCT method for CO ($\nu = 0$) in

this model (Figure 2 (a)). As a result of the overestimate of the $v = 0$ reaction probabilities, the QCT method yields too small a difference between CO ($v = 0$) and CO ($v = 1$), which is particularly important for the 6D case, and these results are not included in Figure 3. The fact that the TDWP 6D reaction probabilities for CO ($v = 1$) are considerably larger than those for CO ($v = 0$) is in contradiction with criterion (i) above for CO to act as a spectator. In conclusion, none of the two criteria defined above are fulfilled, which leads to the conclusion that the CO vibration is not a spectator in the OH + CO reaction. A full 6D calculation is required to describe correctly the reaction of CO ($v = 1$), while for CO ($v = 0$) a PA5D calculation is sufficiently accurate as far as the average trend in reaction probabilities is concerned.

Another point that arises concerning the 6D calculations in Figure 3 (a) is the efficiency of CO vibrational excitation at promoting the OH + CO reaction. Since the quantum of vibrational excitation in CO (0.27 eV) is much larger than the observed shift between the CO ($v = 1$) and CO ($v = 0$) curves in Figure 3 (a) (0.12−0.15 eV), one can conclude that at the same total energy, translational energy is more efficient than vibrational energy of CO in promoting the OH + CO reaction. One can define the vibrational efficacy, Θ, of the reaction for excitation of the CO bond as

$$\Theta = \{(E_{trans,\,CO\,(v=0)}(R) - E_{trans,CO\,(v=1)}(R))\}/\{(E_{vib,CO\,(v=1)} - E_{vib,CO\,(v=0)})\}$$

where R is a given value of the reaction probability. Thus, the vibrational efficacy is the ratio of the shift in translational energy that makes the reaction probabilities of CO ($v = 0$) and CO ($v = 1$) approximately equal and the difference in the vibrational energies of gas-phase CO for these two states. According to this definition, the vibrational efficacy for vibrational excitation of CO is around 50%, depending somewhat on the translational energy (see Figure 3 (a)).

2. Reaction Mechanism for Vibrationally Excited CO. The fact that the difference between the reactions of CO ($v = 1$) and CO ($v = 0$) in the 6D model is much larger than in the PA5D model (Figure 3) suggests that the reaction mechanism through which the CO ($v = 1$) reaction proceeds differs depending on the model used. In the PA5D model, the CO bond is treated diabatically, meaning that the CO vibrational wave function does not change along the reaction path. This yields very little, if any, possibility to describe the possible effects of vibrational deexcitation of the CO bond. In fact, the diabatic picture will be close to an uncoupled vibrationally adiabatic picture if the CO bond length is more or less conserved along the reaction path (as is the case here) and if the same is true for the force constant describing the CO vibration. In contrast, in the 6D model vibrational excitation or deexcitation of the CO bond, as well as coupling to the other degrees of freedom of the system, can also occur.

To gain further insight into the reaction mechanism, we have also constructed an adiabatic 5 + 1D model, in which we first solve for the perturbed reactant CO vibration at each point describing CO in HOCO to obtain an effective 5D PES. The adiabatic 5 + 1D model has been compared to the diabatic PA5D model, and to the energies obtained adding the vibrational energies of the normal mode most similar to the nonreactive CO stretch in the $v = 0$ and $v = 1$ states to the 6D potential, along the projected reaction path. The results are shown in Figure 4 and Table 2.

As seen in Figure 4, CO ($v = 1$) can release more vibrational energy than CO ($v = 0$) in going from reactants to the exit

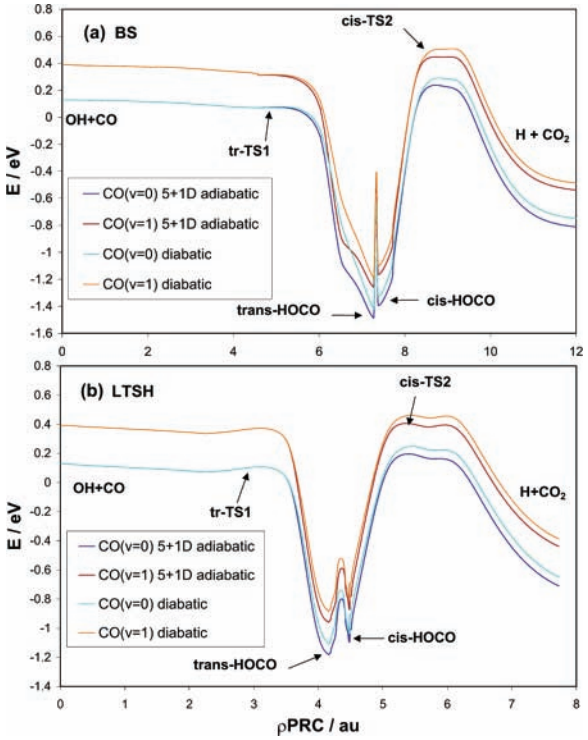

Figure 4. Variation of the energy along the projected reaction coordinate (see text) for the diabatic model and for the adiabatic 5 + 1D model. The curves for the reaction of CO ($v = 0$) are represented in blue tones and those for the reaction of CO ($v = 1$) in red tones, for the BS PES **(a)**, and for the LTSH PES **(b)**. The approximate location of stationary points is indicated in the plots.

channel barrier. This extra energy is very similar in the diabatic (0.050 eV) and adiabatic 5 + 1D (0.055 eV) models and for the BS and LTSH PES's, and slightly larger in a normal mode approximation (0.070−0.075 eV); see Table 2. For the diabatic approximation, the energy difference is in very good agreement with the shift of the reaction probability curve of CO ($v = 1$) to lower energies relative to that of CO ($v = 0$), as obtained in our diabatic (PA5D) model (Figure 3 (b)). The latter result indicates that the CO vibration has an essentially local character along the reaction path up to the exit channel TS, thereby justifying the use of a separable approximation as in the PA5D and adiabatic 5 + 1D models. A similar argument based on the change in the frequency of the non- reactive bond along the reaction coordinate has been invoked to explain the different reactivity of the ground and first excited states of OH and CN in the OH + H_2[59] and H_2 + CN[79] reactions, respectively, although the effect was found to be smaller. The corresponding shift for the adiabatic 5 + 1D model is expected to be very similar. The shifts observed here for the PA5D model (0.050 eV, Figure 3 (b)) and predicted by our analysis for the adiabatic 5 + 1D model (0.055 eV) are much smaller than that found in the 6D model (in the range 0.12−0.15 eV, Figure 3 (a)). The much larger difference observed in the 6D model must therefore be due to a substantial part of the $v = 1$ reacting CO molecules losing a full quantum of CO vibrational energy before the exit channel barrier is reached, and transfer of a large part of this energy along the reaction path. Note that vibrational deexcitation has been found to be largely favored in reactions that form collision complexes.[80] The reaction mechanism can be classified as both vibrationally nondiabatic and vibrationally nonadiabatic, or as vibrationally inelastic. In the rest of the paper, we adopt the latter terminology for the reaction mechanism.

TABLE 2: Energy of Stationary Points on the BS and LTSH Potential Surfaces Obtained with the Separable Adiabatic 5+1D, the Diabatic, and the Normal Mode Models (See Text)

BS PES

		OH + CO	trans-HO·C O	cis-H·OCO	cis-H·OCO−OH + CO difference
adiabatic 5 + 1D	$\nu = 0$	0.134	0.074	0.237	0.103
	$\nu = 1$	0.398	0.308	0.447	0.049
diabatic	$\nu = 0$	0.134	0.077	0.288	0.154
	$\nu = 1$	0.398	0.314	0.501	0.103
normal mode	$\nu = 0$	0.134	0.075	0.230	0.096
	$\nu = 1$	0.398	0.314	0.427	0.029

LTSH PES

		OH + CO	trans-HO·C O	cis-H·OCO	cis-H·OCO−OH + CO difference
adiabatic 5 + 1D	$\nu = 0$	0.134	0.107	0.196	0.062
	$\nu = 1$	0.398	0.372	0.405	0.007
diabatic	$\nu = 0$	0.134	0.107	0.247	0.113
	$\nu = 1$	0.398	0.372	0.460	0.062
normal mode	$\nu = 0$	0.134	0.108	0.164	0.030
	$\nu = 1$	0.398	0.378	0.363	−0.035

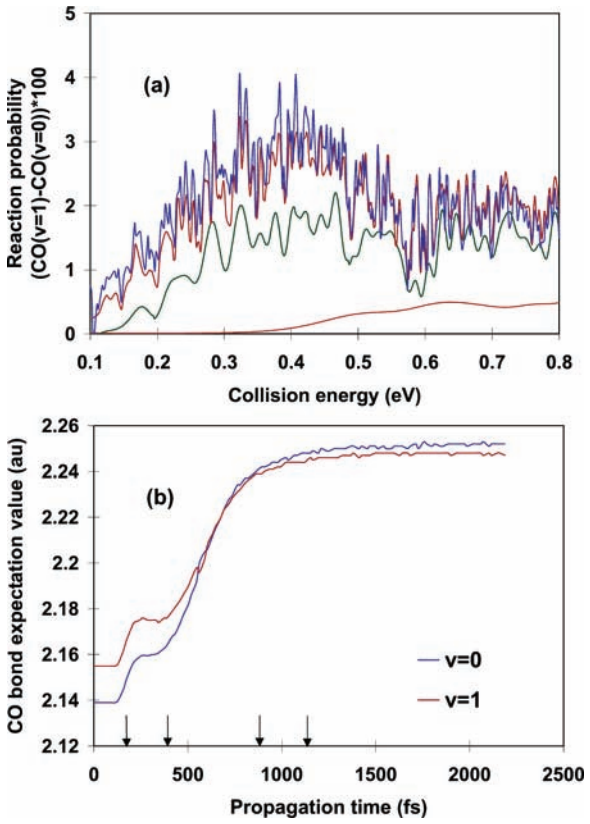

Figure 5. (a) Time evolution of the difference between the 6D reaction probabilities for CO ($\nu = 1$) and CO ($\nu = 0$). The propagation times represented are 220 fs (brown), 440 fs (green), 880 fs (red), and 1170 fs (blue). The energy increment between consecutive data points in the plot is 2.0 meV. **(b)** Time evolution of the CO bond expectation value for CO ($\nu = 0$) (blue line) and CO ($\nu = 1$) (red line). Arrows indicate the propagation times corresponding to the curves in (a).

A clearer view of the dynamics of the reaction of CO ($\nu = 1$) is provided by the time evolution of the TDWP 6D reaction probabilities and of the expectation value of the CO bond distance. Figure 5 (a) shows the difference between the 6D reaction probabilities of CO ($\nu = 1$) and CO ($\nu = 0$) for four different propagation times. As can be seen, the rate of change of the difference in the reactivity of CO ($\nu = 1$) is largest in the early stages of the reaction, decreasing with propagation time and becoming essentially zero after about 0.8 ps. Figure 5 (b) shows the time evolution of the expectation values of the CO bond distance in the reactions of CO ($\nu = 1$) and CO ($\nu = 0$). The expectation value of the CO bond distance for CO ($\nu = 1$) tends toward the value for CO ($\nu = 0$) as propagation time increases. Furthermore, the average CO bond distances become essentially equal at the same propagation time for which the incremental difference in the reaction probabilities of CO ($\nu = 0$) and CO ($\nu = 1$) vanished (≈ 0.8 ps). The increase in the CO bond that is seen in Figure 5 (b) as the wave packet moves into the interaction region is due to the increase of the CO bond distance along the reaction path. The influence of this increase on the reaction dynamics of OH + CO is discussed below. Thus, the information given in Figure 5 is consistent with a picture of the CO ($\nu = 1$) reaction in which for many collisions the CO bond suffers an essentially complete deexcitation early in the reaction, due to vibrationally inelastic interactions along the reaction coordinate. The energy released in the process is either used within about 0.8 ps to surmount the last reaction barrier, or it is randomized within the complex after which there is barely any difference between the reactivity of CO ($\nu = 0$) and CO ($\nu = 1$).

3. Comparison of the Dynamics on the BS and LTSH Potential Surfaces. All the dynamics calculations presented so far were carried out on the BS PES. As explained above, the most recent (LTSH) PES represents an improvement over the BS PES, which, according to previous TDWP studies,[57,58] leads to rather different reaction probabilities than those predicted by the BS PES for the reaction of CO ($\nu = 0$). Thus, it seems important to assess if the behavior of the OH + CO reaction with respect to the CO vibration found above for the BS PES would be qualitatively the same for the LTSH PES. Due to the large computational cost involved, a full 6D TDWP study could not be carried out for the latter potential surface. Instead, we adopted the strategy of comparing the TDWP and QCT calculations for the BS PES, and from this comparison and additional QCT and PA5D TDWP calculations for the LTSH PES inferring what the 6D TDWP results are expected to be for this potential surface.

Results for the LTSH potential surface are presented in Figures 6 and 7. First, a separate comparison is made of the reactivity of CO ($\nu = 0$) (Figure 6 (a)) and CO ($\nu = 1$) (Figure 6 (b)) in the 6D and PA5D models. Figure 6 (a) shows that the PA5D QCT results for CO ($\nu = 0$) compare quite well with the PA5D TDWP results already presented elsewhere.[58] Also,

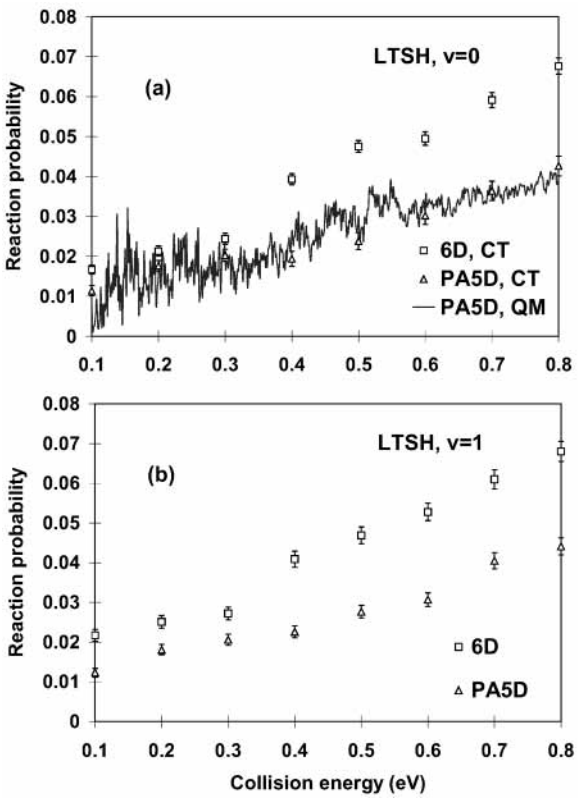

Figure 6. Reaction probabilities for the LTSH PES. **(a)** Results for CO ($\nu = 0$) in the 6D model (open squares for QCT results (CT)), and in the PA5D model (TDWP results in blue, open triangles for QCT results). **(b)** QCT results for CO ($\nu = 1$) in the 6D model (open squares), and in the PA5D model (open triangles). The energy increment between consecutive data points in the TDWP calculation is 0.32 meV. Error bars correspond to two standard deviations for 10 000 trajectories/energy.

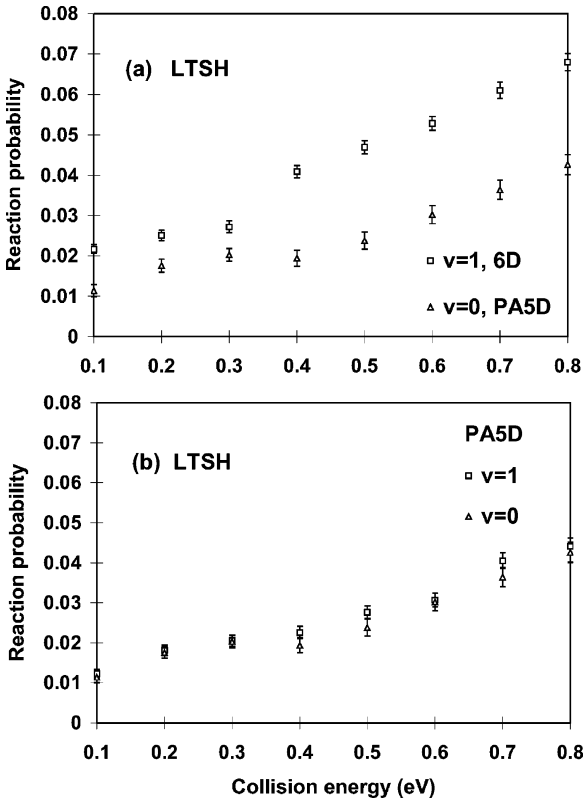

Figure 7. Reaction probabilities for the LTSH PES. **(a)** QCT results in the PA5D model for CO ($\nu = 0$) (open triangles), and in the 6D model for CO ($\nu = 1$) (open squares). **(b)** QCT results in the PA5D model for CO ($\nu = 0$) (open triangles), and for CO ($\nu = 1$) (open squares). Error bars correspond to two standard deviations for 10000 trajectories/energy.

the QCT reaction probabilities are much larger in the 6D model than in the PA5D model. It seems reasonable to expect that the results of the 6D model calculation will be much too large compared to those that would be obtained in a TDWP calculation, this being a consequence of ZPE effects as was found for the BS PES (Figure 2 (a)). Therefore, we will not further discuss the 6D QCT result for CO ($\nu = 0$) and the LTSH PES. The QCT calculations for CO ($\nu = 1$) presented in Figure 6 (b) show the same trend as for the BS PES, that is, much larger reaction probabilities in the 6D model than in the PA5D model at all collision energies. We do trust this result, because the QCT model gave quite good results for the reaction of CO ($\nu = 1$) in both the 6D and the PA5D model for the BS PES.

A further comparison of the QCT results for the LTSH PES is shown in Figure 7. In Figure 7 (a), the QCT results that should give the best predictions of the quantum reaction probabilities for CO ($\nu = 1$) and CO ($\nu = 0$), that is, the 6D model for CO ($\nu = 1$) and the PA5D model for CO ($\nu = 0$), are presented. Essentially, their difference is as large as that found between the 6D and PA5D QCT results for CO ($\nu = 1$) (Figure 6 (b)), due to the fact that the PA5D QCT results are very similar for CO ($\nu = 0$) and CO ($\nu = 1$), with slightly larger reaction probabilities for CO ($\nu = 1$) (Figure 7 (b)). For energies greater than 0.3 eV, Figure 7 (a) shows that the nonreactive CO bond does clearly not act as a spectator. For energies smaller than 0.3 eV, the QCT calculations also suggest that CO does not act as a spectator. However, it would be desirable to also have TDWP results available for this range of energies, to rule out any uncertainty caused by the inaccuracies of the QCT method, on one hand, and any uncertainty caused by the difference between the CO ($\nu = 1$) and CO ($\nu = 0$) results being relatively small, on the other hand. At the same time, we firmly believe that the additional TDWP results would confirm the QCT results for these lower energies, since there is no reason to expect that the CO vibration would affect the reaction through different mechanisms for the two energy regions. We expect the vibrationally inelastic mechanism that applies for the BS PES to also be valid for the LTSH PES.

The trends shown in Figures 6 and 7 regarding the behavior of the CO ($\nu = 0$) and CO ($\nu = 1$) reactions in the 6D and the PA5D model for the LTSH PES are in a qualitatively good agreement with those already presented for the BS PES (Figures 2 and 3). As noted above, a comparison of the TDWP and QCT results for the BS PES strongly suggests that the QCT method is able to provide a good description of the reaction of CO ($\nu = 1$) in both the 6D and the PA5D model (Figure 2 (b)), and that it also provides a good description of the reactivity of CO ($\nu = 0$) in the PA5D model, but not in the 6D model (Figure 2 (a)).

All the above results taken together therefore strongly suggest that the TDWP method would also find a larger reactivity for CO ($\nu = 1$) than for CO ($\nu = 0$) in the 6D model (Figure 7 (a)), and a larger reactivity for CO ($\nu = 1$) in the 6D model than in the PA5D model, for the LTSH PES. Therefore, we would expect the outcome of TDWP calculations on the LTSH PES to be that the CO bond does not behave as a spectator also for this most recent potential surface.

To gain some understanding of the relation between the dynamical results presented above and the differences between

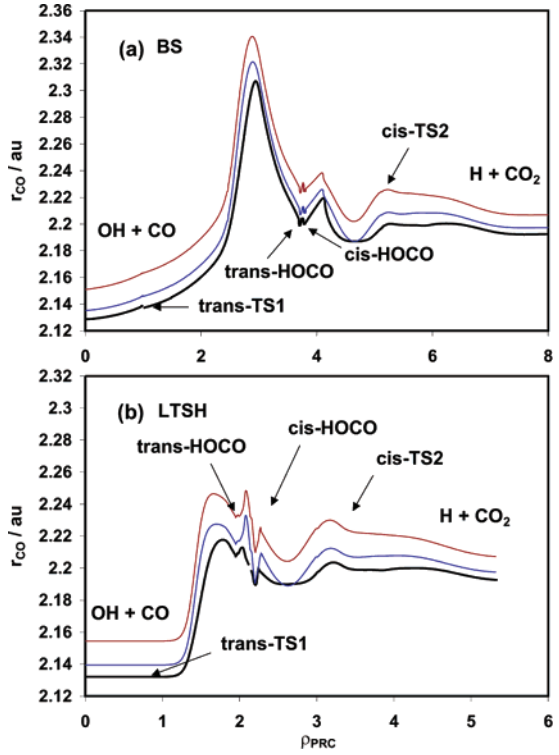

Figure 8. Variation of the CO bond distance and of its expectation values in the $\nu = 0$ and $\nu = 1$ vibrational states along the projected reaction coordinate (see text). **(a)** BS PES, and **(b)** LTSH PES. The approximate location of stationary points is indicated in the plots.

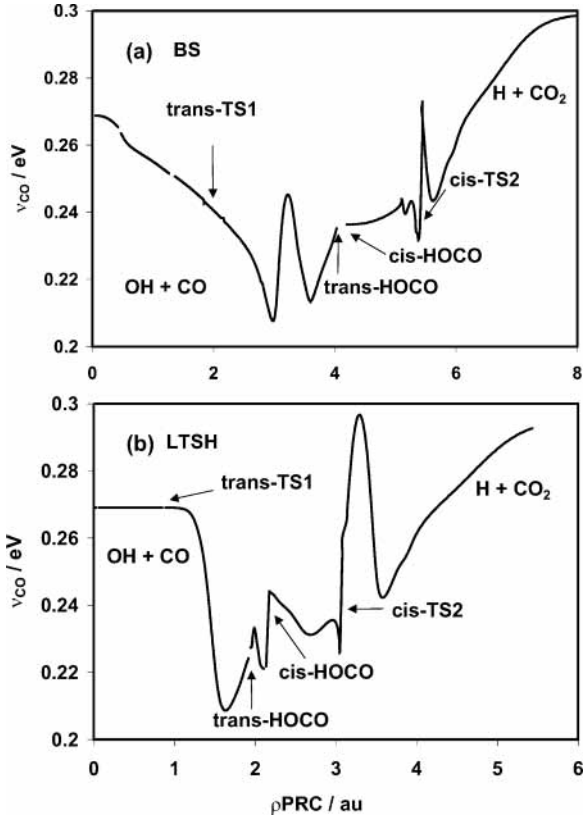

Figure 9. Variation of the CO frequency along the projected reaction coordinate (see text). **(a)** BS PES, and **(b)** LTSH PES. The approximate location of stationary points is indicated in the plots.

the underlying potential surfaces, we have carried out an analysis of the description of the CO bond distance and frequency along the reaction path in the two different potential surfaces. To this aim, the intrinsic reaction coordinate (IRC) was determined by integrating the defining differential equation downhill from the relevant transition states using the POLYRATE 8.5 reaction dynamics program.[81] Figure 8 presents plots of the CO bond distance and of its expectation value in the $\nu = 0$ and $\nu = 1$ vibrational states versus a reduced reaction coordinate ρ_{PRC}, defined as the distance along the IRC projected onto the (R, r_{OH}) reactant Jacobi coordinates, for the BS PES (Figure 8 (a)) and for the LTSH PES (Figure 8 (b)). The distance measured in these Jacobi coordinates is expected to be a good approximation to the true reaction coordinate. As shown in the plots, the CO distance presents a pronounced maximum between the entrance channel barrier and the HOCO minimum for the BS PES (Figure 8 (a)), and a much less prominent maximum in the more recent LTSH PES (Figure 8 (b)). The presence of this pronounced maximum is an unphysical feature of the BS PES, and the question naturally arises as to its possible influence on the reactivity. However, as discussed above, our 6D QCT results for CO ($\nu = 1$) and PA5D QCT results for CO ($\nu = 0$) for the LTSH surface also predict a large difference between the reactivity of CO ($\nu = 1$) and CO ($\nu = 0$) for this surface, which does not contain the pronounced maximum referred to above. The difference observed for the BS PES should therefore not be due to the artifact in the PES, but rather to the same physics as present in the more recent LTSH PES. In both PES's, a sharp increase in the CO bond distance with ρ_{PRC} is observed between the entrance channel barrier and the HOCO minimum, which is however exaggerated in the BS PES. This sharp increase could well lead to vibrationally inelastic energy transfer from the CO vibration to motion along the reaction path, thereby explaining the enhanced reactivity of CO ($\nu = 1$).

It is also interesting to study the relation of Figure 8 with Figure 5 (b) above, which showed the evolution of the average CO bond distance as a function of propagation time in the TDWP calculations. In Figure 8 (a), the CO expectation values for $\nu = 1$ and $\nu = 0$ in separate reactants are 2.135 and 2.151 bohr, respectively, in good agreement with the average CO bond distance at the start of the propagation in Figure 5 (b). For both the CO ($\nu = 0$) and the CO ($\nu = 1$) reaction, the average CO distance increases until a plateau is reached at ≈0.8 ps. Figure 8 (a) shows that in an adiabatic picture a larger average value of the CO distance would be expected for CO ($\nu = 1$) than for CO ($\nu = 0$) throughout the reaction, in contrast to what is observed in Figure 5 (b). This is again consistent with an inelastic mechanism in which the vibrational quantum in CO ($\nu = 1$) is lost during the reaction, after which the evolution of the average CO distance with respect to time is the same as for the ground state (CO ($\nu = 0$)) reaction.

Figure 9 presents plots of the vibrational frequency of CO as a function of the same reduced reaction coordinate as before. In general, the CO frequency tends to decrease, in accordance with the increase in the CO distance as the reaction proceeds to products. The maximum that is observed beyond the exit channel barrier (cis-TS2) is most likely due to the recoupling of the HOCO normal modes as the nonreactive CO bond becomes part of the product CO_2 molecule, and is not expected to have an important effect on the reaction probabilities due to the exothermicity of the reaction.

Some experimental studies comparing the reactivity of CO ($\nu = 0$) and CO ($\nu = 1$) have been reported.[37] In these studies it has been inferred that the rate constant for CO ($\nu = 1$) is somewhat smaller than for CO ($\nu = 0$), or, at any rate, that vibrational excitation of CO has a small effect on the reaction. However, it is difficult to make a meaningful comparison to

these data, since the experimental error bars are larger than the measured difference between the rate constants of the two reactions. As an example, the error bars for a CO vibrational temperature of 298 K are four times larger than the observed difference between the rate constants at CO vibrational temperatures of 298 and 1400 K.[37] Furthermore, for a meaningful comparison with these data, theoretical results would be also required for lower energies than here presented, and the comparison would also be preferably based on theoretical results for $J > 0$.

Conclusions

A quantum and quasiclassical reaction dynamics study of the effect of the vibrational excitation of the CO bond on the OH + CO → H + CO_2 reaction has been presented. It has been found that the CO ($\nu = 1$) vibrationally excited state presents a significantly larger reactivity than the CO ($\nu = 0$) state in the TDWP calculations on the BS PES. The fact that the increase in the reaction probability is larger for the 6D model than for the PA5D model has been explained by an important contribution of a vibrationally inelastic mechanism in the reaction of CO ($\nu = 1$), which can only be accounted for in the 6D model. This reaction mechanism is further supported by the inability of an adiabatic 5 + 1D model to account for the energy shift observed between the CO ($\nu = 1$) and CO ($\nu = 0$) reactions in the 6D model. Therefore, models based on an effective 5D potential are not able to afford a correct qualitative and quantitative description of the dynamics of CO ($\nu = 1$), and a 6D model is required for this reaction. In contrast, previous TDWP calculations on the reaction of CO ($\nu = 0$) had shown that this reaction can be described quite well with the PA5D model.

A comparison of QCT and TDWP results for the BS PES shows that the QCT method is able to reproduce the TDWP results for CO ($\nu = 1$) quite well, in both the 6D and the PA5D model. Furthermore, the QCT method affords a good description of the reaction of CO ($\nu = 0$) in the PA5D model, but not in the 6D model (probably due to zero-point energy conservation problems), for the same PES. An important point arising from this comparison and from the comparison of 6D and PA5D TDWP results for CO ($\nu = 0$) is that 6D QCT results for CO ($\nu = 1$) and PA5D QCT results for CO ($\nu = 0$) may be used to infer the quantum mechanical reactivity of CO ($\nu = 1$) and CO ($\nu = 0$), respectively.

An analysis of the reaction probability curves in the 6D CO ($\nu = 0$) and CO ($\nu = 1$) TDWP calculations with respect to wave packet propagation time reveals that their difference grows during the early stage of the reaction, attaining an essentially constant value at longer propagation times. This behavior correlates with the time evolution of the difference between the expectation values of the CO bond distance in the CO ($\nu = 0$) and CO ($\nu = 1$) reactions, further confirming that vibrationally inelastic effects in CO ($\nu = 1$) are the main cause of the increased reactivity of this state when compared to CO ($\nu = 0$).

Additional QCT calculations were performed to assess whether the conclusions arrived at in the TDWP calculations on the BS PES would also hold for the LTSH PES. The 6D QCT reaction probabilities for CO ($\nu = 1$) were much larger than the PA5D reaction probabilities for CO ($\nu = 0$). Because these sets of results are expected to form accurate predictions of 6D quantum dynamical reaction probabilities for CO ($\nu = 1$) and CO ($\nu = 0$), respectively, it was concluded that the reactivity of CO ($\nu = 1$) should also be much larger than that of CO ($\nu = 0$) for the LTSH PES. Similarly, the QCT prediction for the LTSH PES, that 6D reaction probabilities should be much larger than PA5D reaction probabilities for CO ($\nu = 1$), is also expected to hold in quantum dynamics.

The main conclusion of this study is that the dynamical behavior of the CO bond in the OH + CO reaction is not consistent with a spectator picture, in two related senses: (a) for CO ($\nu = 1$), the 6D reaction probabilities are significantly different from the PA5D ones; and (b) in the 6D model, the CO ($\nu = 1$) reaction probabilities are much larger than the CO ($\nu = 0$) ones, especially at low collision energies. The above conclusion was based on quantum dynamics results for the BS PES, but our QCT results for the LTSH PES strongly suggest that the conclusion that CO does not act as a spectator should also hold for the LTSH PES.

Acknowledgment. The authors thank G.C. Schatz for providing the potential surfaces used in this work and for fruitful discussions, W.L. Hase for providing us with his VENUS'96 code, and D.G. Truhlar for making his POLYRATE (version 8.5) program available to us. We also thank CW/NWO for Jonge Chemici and CW program grants. The TDWP calculations were made possible through a Dutch Computing Challenge grant by the National Computing Facilities foundation (NCF).

References and Notes

(1) Röckmann, T.; Brenninkmeijer, C. A. M.; Saueressig, G.; Bergamaschi, P.; Crowley, J. N.; Fischer, H.; Crutzen, P. J. *Science* **1996**, *281*, 544.

(2) Warnatz, J. *Combustion Chemistry*; Gardiner W. C., Jr., Ed.; Springer: New York, 1984; p 197.

(3) van Dishoeck, E. F. et al. *Astron. Astrophys*. **1996**, *315*, L349.

(4) Mozurkewich, M.; Benson, S. W. *J. Phys. Chem.* **1984**, *88*, 6435.

(5) Brunning, J.; Derbyshire, D. W.; Smith, I. W. M.; Williams, M. D. *J. Chem. Soc., Faraday Trans*. **1988**, *2 84*, 105.

(6) Sonnenfroh, D. M.; Macdonald, R. G.; Liu, K. *J. Chem. Phys.* **1991**, *94*, 6508.

(7) Frost, M. J.; Sharkey, P.; Smith, I. W. M. *Faraday Discuss. Chem. Soc*. **1991**, *91*, 305.

(8) Alagia, M.; Balucani, N.; Casavecchia, P.; Stranges, D.; Volpi, G. G. *J. Chem. Phys.* **1993**, *98*, 8341.

(9) Kim, E. H.; Bradforth, S. E.; Arnold, D. W.; Metz, R. B.; Neumark, D. M. *J. Chem. Phys.* **1995**, *103*, 7801.

(10) Koppe, S.; Laurent, T.; Volpp, H. R.; Wolfrum, J.; Naik, P. D. *Proceedings of the Twenty-sixth International Symposium on Combustion*; The Combustion Institute: Pittsburgh, 1996; p 489.

(11) Fulle, D.; Hamann, H. F.; Hippler, H.; Troe, J. *J. Chem. Phys.* **1996**, *105*, 983, and references therein.

(12) Golden, D. M.; Smith, G. P.; McEwen, A. B.; Yu, C. L.; Eiteneer, B.; Frenklach, M.; Vaghjiani, G. L.; Ravishankara, A. R.; Tully, F. P. *J. Phys. Chem. A* **1998**, *102*, 8598.

(13) van Beek, M. C.; Schreel, K.; ter Meulen, J. J. *J. Chem. Phys.* **1998**, *109*, 1302.

(14) Brouard, M.; Hughes, D. W.; Kalogerakis, K. S.; Simons, J. P. *J. Phys. Chem. A* **1998**, *102*, 9559.

(15) Brouard, M.; Hughes, D. W.; Kalogerakis, K. S.; Simons, J. P. *J. Chem. Phys*. **2000**, *112*, 4557.

(16) Brouard, M.; Burak, I.; Hughes, D. W.; Kalogerakis, K. S.; Simons, J. P.; Stavros, V. *J. Chem. Phys*. **2000**, *113*, 3173.

(17) Lester, M. I.; Pond, B. V.; Anderson, D. T.; Harding, L. B.; Wagner, A. F. *J. Chem. Phys.* **2000**, *113*, 9889.

(18) Lester, M. I.; Pond, B. V.; Marshall, M. D.; Anderson, D. T.; Harding, L. B.; Wagner, A. F. *Faraday Discuss*. **2001**, *118*, 373.

(19) Clements, T. G.; Continetti, R. E. *J. Chem. Phys*. **2001**, *115*, 5345.

(20) van Beek, M. C.; ter Meulen, J. J. *J. Chem. Phys*. **2001**, *115*, 1843.

(21) Greenslade, M. E.; Tsiouris, M.; Bonn, R. T.; Lester, M. I. *Chem. Phys. Lett*. **2002**, *354*, 203.

(22) Clements, T. G.; Continetti, R. E.; Francisco, J. S. *J. Chem. Phys*. **2002**, *117*, 1.

(23) Marshall, M. D.; Pond, B. V.; Lester, M. I. *J. Chem. Phys*. **2003**, *118*, 1196.

(24) Pond, B. V.; Lester, M. I. *J. Chem. Phys.* **2003**, *118*, 2223.

(25) Smith, I. W. M.; Zellner, R. *J. Chem. Soc. Far. Trans*. **1973**, *2 69*, 1617.

(26) Ruscic, B.; Schwatz, M.; Berkowitz, J. *J. Chem. Phys*. **1989**, *91*, 6780.
(27) Radford, H. E.; Wei, W.; Sears, T. J. *J. Chem. Phys.* **1992**, *97*, 3989.
(28) Petty, J. T.; Moore, C. B. *J. Chem. Phys.* **1993**, *99*, 47.
(29) Sears, T. J.; Radford, H. E.; Moore, M. A. *J. Chem. Phys*. **1993**, *98*, 6624.
(30) Miyoshi, A.; Matsui, H.; Washida, N. *J. Chem. Phys*. **1994**, *100*, 3532.
(31) Ruscic, B.; Litorja, M. *Chem. Phys. Lett*. **2000**, *316*, 45.
(32) Milligan, D. E.; Jacox, M. E. *J. Chem. Phys.* **1971**, *54*, 927.
(33) Jacox, M. E. *J. Chem. Phys*. **1988**, *88*, 4598.
(34) Forney, D.; Jacox, M. E.; Thompson, W. E. *J. Chem. Phys*. **2003**, *119*, 10814.
(35) Kudla, K.; Schatz, G. C.; Wagner, A. F. *J. Chem. Phys.* **1991**, *95*, 1635.
(36) Zhu, R. S.; Diau, E. G. W.; Lin, M. C.; Mebel, A. M. *J. Phys. Chem. A* **2001**, *105*, 11249.
(37) Dreier, T.; Wolfrum, J. *Proceedings of the Eighteenth International Symposium on Combustion*; The Combustion Institute: Pittsburgh, 1981; p 801.
(38) Wooldridge, M. S.; Hanson, R. K.; Bowman, C. T. *Proceedings of the Twenty-Fifth International Symposium on Combustion*; The Combustion Institute: Pittsburgh, 1994; p 741.
(39) Schatz, G. C.; Fitzcharles, M. S.; Harding, L. B. *Faraday Discuss. Chem. Soc.* **1987**, *84*, 359.
(40) Bradley, K. S.; Schatz, G. C. *J. Chem. Phys*. **1997**, *106*, 8464.
(41) Yu, H.-G.; Muckerman, J. T.; Sears, T. J. *Chem. Phys. Lett*. **2001**, *349*, 547.
(42) Lakin, M. J.; Troya, D.; Schatz, G. C.; Harding, L. B. *J. Chem. Phys*. **2003**, *119*, 5848.
(43) Kudla, K.; Koures, A. G.; Harding, L. B.; Schatz, G. C. *J. Chem. Phys.* **1992**, *96*, 7465.
(44) Schatz, G. C.; Dyck, J. *Chem. Phys. Lett*. **1992**, *188*, 11.
(45) Clary, D. C.; Schatz, G. C. *J. Chem. Phys.* **1993**, *99*, 4578.
(46) Hernández, M. I.; Clary, D. C. *J. Chem. Phys*. **1994**, *101*, 2779.
(47) Goldfield, E. M.; Gray, S. K.; Schatz, G. C. *J. Chem. Phys.* **1995**, *102*, 8807.
(48) Zhang, D. H.; Zhang, J. Z. H. *J. Chem. Phys.* **1995**, *103*, 6512.
(49) Dzegilenko, F. N.; Bowman, J. M. *J. Chem. Phys.* **1996**, *105*, 2280.
(50) Dzegilenko, F. N.; Bowman, J. M. *J. Chem. Phys*. **1998**, *108*, 511.
(51) McCormack, D. A.; Kroes, G.-J. *J. Chem. Phys*. **2002**, *116*, 4184.
(52) Yu, H.-G.; Muckerman, J. T. *J. Chem. Phys.* **2002**, *117*, 11139.
(53) Balakrishnan, N.; Billing, G. D. *J. Chem. Phys*. **1996**, *104*, 4005.
(54) Feilberg, K. L.; Billing, G. D.; Johnson, M. S. *J. Phys. Chem. A* **2001**, *105*, 11171.
(55) Billing, G. D.; Muckerman, J. T.; Yu, H.-G. *J. Chem. Phys*. **2002**, *117*, 4755.
(56) McCormack, D. A.; Kroes, G.-J. *Chem. Phys. Lett*. **2002**, *352*, 281; **2003**, *373*, 648 (Erratum).
(57) Medvedev, D. M.; Gray, S. K.; Goldfield, E. M.; Lakin, M. J.; Troya, D.; Schatz, G. C. *J. Chem. Phys*. **2004**, *120*, 1231.
(58) Valero, R.; McCormack, D. A.; Kroes, G.-J. *J. Chem. Phys*. **2004**, *120*, 4263.
(59) Zhang, D. H.; Zhang, J. Z. H. *J. Chem. Phys.* **1994**, *101*, 1146.
(60) Zhu, W.; Zhang, J. Z. H.; Zhang, Y. C.; Zhang, Y. B.; Zhan, L. X.; Zhang, S. L.; Zhang D. H. *J. Chem. Phys.* **1998**, *108*, 3509.
(61) Walch, S. P.; Dunning, T. H., Jr. *J. Chem. Phys.* **1980**, *72*, 1303.
(62) Szichman, H.; Last, I.; Baer, M. *J. Phys. Chem.* **1994**, *98*, 828.
(63) Bethardy, G. A.; Wagner, A. F.; Schatz, G. C.; ter Horst, M. A. *J. Chem. Phys*. **1997**, *106*, 6001.
(64) Neuhauser, D.; Baer, M. *J. Chem. Phys*. **1989**, *91*, 4651.
(65) Light, J.; Hamilton, I.; Lill, J. *J. Chem. Phys*. **1985**, *82*, 1400.
(66) Zhang, J. Z. H. *Theory and Application of Quantum Molecular Dynamics*; World Scientific: Singapore, 1999.
(67) Corey, G. C.; Tromp, J. W. *J. Chem. Phys*. **1995**, *103*, 1812.
(68) Fleck, J. A., Jr.; Morris, J. R.; Feit, M. D. *Appl. Phys*. **1976**, *10*, 129.
(69) Vibók, Á.; Balint-Kurti, G. G. *J. Phys. Chem.* **1992**, *96*, 8712.
(70) Neuhauser, D. H.; Baer, M.; Judson, R. S.; Kouri, D. *J. Comput. Phys. Commun.* **1991**, *63*, 460.
(71) Information on OpenMP is available at the Web site http://www.openmp.org
(72) Hase, W. L. et al., Quantum Chemistry Program Exchange **1996**, *16*, 671.
(73) Hase, W. L.; Darling, C. L.; Zhu, L. *J. Chem. Phys.* **1992**, *96*, 8295.
(74) Aoiz, F. J.; Bañares, L.; Díez-Rojo, T.; Herrero, V. J.; Sáez-Rábanos, V. *J. Phys. Chem.* **1996**, *100*, 4071.
(75) Aoiz, F. J.; Martínez, M. T.; Menéndez, M.; Sáez-Rábanos, V.; Verdasco, E. *Chem. Phys. Lett.* **1999**, *299*, 250.
(76) Aoiz, F. J.; Verdasco, E.; Sáez Rábanos, V.; Loesch, H. J.; Menéndez, M.; Stienkemeier, F. *Phys. Chem. Chem. Phys.* **2000**, *2*, 541.
(77) Schatz, G. C.; Lendvay, G. *J. Chem. Phys.* **1997**, *106*, 3548.
(78) Schatz, G. C. *J. Chem. Phys*. **1983**, *79*, 5386.
(79) Takayanagi, T.; Schatz, G. C. *J. Chem. Phys*. **1997**, *106*, 3227.
(80) Smith, I. W. M. *J. Chem. Soc., Faraday Trans.* **1997**, *93*, 3741.
(81) Corchado, J. C.; Chuang, Y.-Y.; Fast, P. L.; Villà, J.; Hu, W.-P.; Liu, Y.-P.; Lynch, G. C.; Nguyen, K. A.; Jackels, C. F.; Melissas, V. S.; Lynch, B. J.; Rossi, I.; Coitiño, E. L.; Fernández-Ramos, A.; Steckler, R.; Garrett, B. C.; Isaacson, A. D.; Truhlar, D. G. *POLYRATE*, version 8.5; University of Minnesota: Minneapolis, 2000.